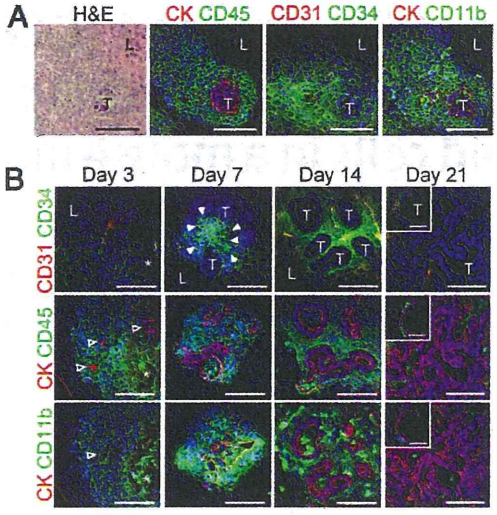

Fig. 1. Accumulation of iMCs around disseminated cancer cells in the liver. (*A*) A metastatic focus in the liver stained with H&E (*Far Left*). Serial sections were immunostained for pan-cytokeratin (CK), CD45, CD31, CD34, and CD11b. T, metastasizing tumor; L, adjacent normal liver. (Scale bars, 100 μm.) (*B*) Liver metastasis foci dissected at days 3, 7, 14, and 21 postinjection. Open arrowheads, disseminated tumor cells; filled arrowheads, a cluster of the iMCs; asterisks, a necrotic area. T, tumor glands; L, adjacent normal liver. (*Insets*) A representative carcinoma cyst. (Scale bars, 100 μm.)

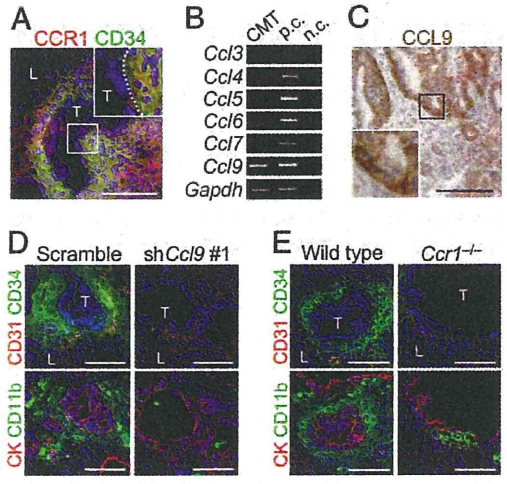

Fig. 2. Inactivation of CCL9-CCR1 signaling blocks accumulation of the iMCs in the liver. (*A*) A metastatic focus in the liver immunostained for CCR1 and CD34. (*Inset*) A higher magnification of the boxed area. T, tumor; L, liver. (Scale bar, 100 μm.) (*B*) Expression of mRNAs for CCR1 ligands determined by RT-PCR. Total RNA was isolated from cultured CMT93 cells. Total RNA from intestinal polyps of *Apc/Smad4* mice was used as a control (p.c.). Negative controls (n.c.) had distilled water instead of RNA. (*C*) A metastatic focus in the liver immunostained for CCL9 (brown DAB staining with hematoxylin counterstaining). (*Inset*) A higher magnification of the boxed area. (Scale bar, 100 μm.) (*D*) Liver metastasis foci in mice injected with CMT93 cells expressing scramble RNA (Scramble) and shRNA against *Ccl9* (sh*Ccl9*#1). Serial sections were immunostained for CK, CD31 and the iMC markers (CD34 and CD11b). T, tumor; L, liver. (Scale bars, 100 μm.) (*E*) Liver metastasis foci in wild-type and *Ccr1*$^{-/-}$ mice injected with CMT93 cells. (Scale bars, 100 μm.)

iMCs disappeared from the metastatic lesions where the cancer cells formed massive glands or carcinoma cysts, suggesting the possibility that the iMCs contributed to an early phase of metastatic expansion. As mentioned above, we could not find VEGFR1$^+$ cells in the liver lesions during 2 wk after injection (Fig. S1*A*), although such cells were reported in lung metastatic sites at day 12 after s.c. injection of melanoma cells (8).

Mouse Colon Cancer Cells Secrete CCL9 and Recruit CCR1-Expressing iMCs to the Liver. We next investigated CCR1 expression, another important characteristic of the iMCs. Most iMCs at the metastatic foci expressed CCR1, whereas the cancer epithelium did not (Fig. 2*A*). Because specific ligands activate CCR1 (13) and recruit the iMCs (12), we looked for such ligands that were expressed by the cancer cells. Among them, CMT93 cells expressed only *Ccl9* mRNA but others did not (Fig. 2*B*). Consistently, cultured CMT93 cells secreted CCL9 protein (25 ± 3 pg/10^5 cells) at a similar level to that by intestinal cancer cells from *Apc/Smad4* polyps (37 ± 16 pg/10^5 cells). Immunostaining data also confirmed that metastasized CMT93 cells expressed CCL9 but the surrounding stromal cells did not (Fig. 2*C*).

To assess the importance of CCL9 in iMC accumulation in the liver, we prepared CMT93 derivatives that contained shRNA against *Ccl9* or control scramble RNA. Two constructs of the shRNA, sh*Ccl9*#1 and sh*Ccl9*#2, reduced the CCL9 levels to 25% and 47% of control CMT93-scramble cells, respectively (i.e., 7 ± 1, 14 ± 2, and 29 ± 7 pg/10^5 cells for CMT-sh*Ccl9*#1, CMT-sh*Ccl9*#2, and CMT93-scramble, respectively). As expected, almost all metastatic foci formed by control cells accumulated iMCs markedly. In contrast, such accumulations were not observed in the majority of foci by the CCL9-reduced CMT93 cells (CMT93-sh*Ccl9*#1; Fig. 2*D*). We further injected CMT93 cells into *Ccr1*$^{-/-}$ mice and found that 7 of 10 mice formed no visible metastatic foci in the liver, although the remaining three developed some foci (see below). We therefore examined the minor population of mice for liver metastases, but iMCs were missing around most such lesions (Fig. 2*E*). Collectively, these results suggest that activation of CCR1 by cancer-secreted CCL9 is critical for the iMCs to accumulate at the metastatic foci. As an exception, we found several small metastatic lesions where numerous iMCs accumulated despite the lack of CCR1 (Fig. S2), suggesting a rare alternative mechanism that can recruit iMCs independent of CCR1.

Inactivation of the Mouse CCL9-CCR1 Signaling Blocks Metastatic Expansion of Cancer in the Liver, and Prolongs Host Survival. Because the iMCs helped invasion of primary tumors in the intestines (12), we hypothesized that accumulation of the iMCs could also promote the metastatic expansion of disseminated colon cancer in the liver. We therefore injected luciferase-expressing CMT93 cells into *nu/nu* mice (nude mice), which enabled monitoring of the liver tumors by bioluminescence over time. In mice injected with the parental CMT93 or CMT93-scramble cells, the intensity of bioluminescence began to increase at day 7 postinjection and increased exponentially thereafter (Fig. 3 *A* and *B*). In contrast, such an increase in luminescence was markedly suppressed in mice injected with CMT93-sh*Ccl9*#1 cells, although they showed essentially the same levels of luminescence as control groups up to day 3. Another shRNA construct (sh*Ccl9*#2) showed a similar effect, although at a weaker level than that of sh*Ccl9*#1 (Fig. 3*B*). Of note, all CMT93 derivatives showed essentially the same luciferase activity and proliferation rate in culture. We then injected luciferase-expressing CMT93 cells into the wild-type and *Ccr1*$^{-/-}$ mice. Although all wild-type mice showed marked increases in the luminescence level at day 14 postinjection, such an increase was not observed in 70% (7/10) of *Ccr1*$^{-/-}$ mice (Fig. 3*C*). In these hosts, we did not find any macroscopic foci on liver surfaces (Fig. 3*D*). These results indicate that accumulation of the iMCs via CCL9-CCR1 axis plays a major role in the expansion of liver metastasis foci. Although all mice injected with the CMT93-scramble or parental cells became moribund within 54 d, 60% (3/5) and 20% (2/10) of mice injected with CMT93-sh*Ccl9* #1 and CMT93-sh*Ccl9* #2 cells, respectively,

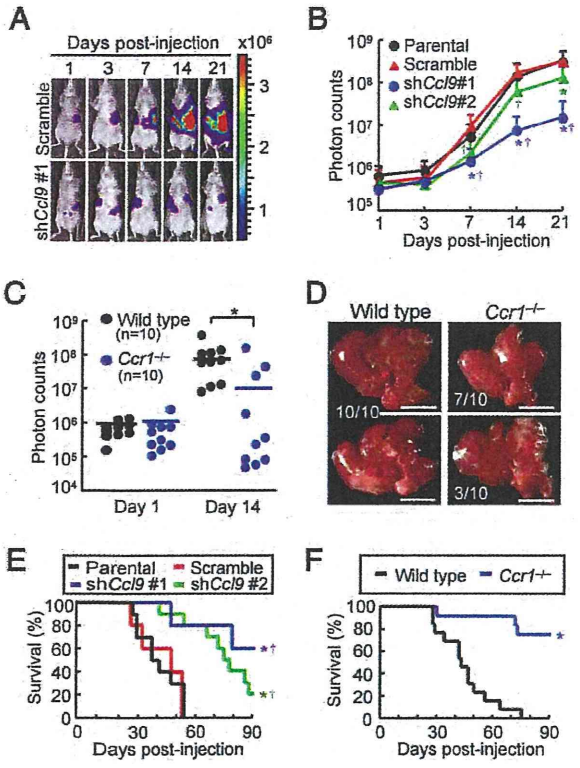

Fig. 3. Blockade of CCL9-CCR1 signaling suppresses expansion of metastatic lesions and prolongs host survival. (*A*) Representative in vivo bioluminescence images of mice injected with luciferase-expressing CMT93 cells that contained scramble RNA (*Upper*) or shRNA against *Ccl9* (*Lower*). Colored scale bar represents intensity of bioluminescence in photons/sec. (*B*) Quantification of metastatic lesions by bioluminescence (photon counts) from luciferase-expressing CMT93 cells (Parental), or their derivatives that contained scramble RNA (Scramble) or shRNA against *Ccl9* (sh*Ccl9*#1 or sh*Ccl9*#2). Results are given as the means ± SD $*P < 0.02$ and $^{\dagger}P < 0.02$ compared with Parental and Scramble, respectively (n = 8–11 mice in each group). (*C*) Quantification of metastatic lesions by bioluminescence from luciferase-expressing CMT93 cells injected into wild-type and *Ccr1*$^{-/-}$ mice. Each circle represents an individual mouse. Horizontal lines show the means of the respective groups. $*P < 0.01$. (*D*) Representative macroscopic views of the liver dissected from wild-type and *Ccr1*$^{-/-}$ mice injected with CMT93 cells. (Scale bars, 10 mm.) (*E*) Kaplan-Meier plot showing survival of wild-type hosts injected with control CMT93 cells (Prnt and Scr) or those containing shRNA constructs against *Ccl9* (sh*Ccl9*#1 or sh*Ccl9*#2). $*P < 0.01$ and $^{\dagger}P < 0.02$ compared with Prnt and Scr, respectively (n = 5–10 mice in each group). (*F*) Survival rates of wild-type and *Ccr1*$^{-/-}$ mice injected with parental CMT93 cells. $*P = 0.0001$ (n = 12–13 mice in each group).

remained alive till the end of analysis (day 90; Fig. 3*E*). Likewise, 75% (9/12) of the tumor-transplanted *Ccr1*$^{-/-}$ mice survived to day 90, in contrast to the wild type that became moribund before day 75 (Fig. 3*F*). These results indicate that inactivation of the CCL9-CCR1 signaling prolongs the survival by blocking early metastatic expansion.

Lack of MMP2 or MMP9 in the Host Mouse Suppresses Expansion of Metastatic Lesions in the Liver. For metastatic expansion in the liver, disseminated cancer cells need to invade the liver parenchyma. We therefore hypothesized that the iMCs promote intrahepatic invasion of disseminated cancer through secretion of proteases. To identify such enzymes, we compared mRNA levels in the metastatic foci between the wild-type and *Ccr1*$^{-/-}$ mice by microarray and RT-PCR (Fig. S3*A*). The results showed more than twofold increases in the levels of *Mmp2*, *Mmp7*, *Mmp9*, and *Mmp13* in the iMC-associated foci in wild-type mice (Fig. S3*B*). In such lesions, MMP2 and MMP9 were expressed in the stromal iMCs, but not in the cancer epithelium (Fig. 4 *A* and *B*), whereas MMP7 and MMP13 were found primarily in the epithelium (Fig. S3*C*). Consistently, MMP2 and MMP9 were absent around the liver foci in *Ccr1*$^{-/-}$ mice where the iMCs were missing, although MMP7 and MMP13 were present (Fig. 4*A* and Fig. S3*C*). We then injected luciferase-expressing CMT93 cells into *Mmp2*$^{-/-}$ mice and found significant reduction in the liver luminescence at day 14, compared with those in *Mmp2*$^{+/+}$ littermates (Fig. 4*C*). Likewise, the luciferase luminescence was much lower in *Mmp9*$^{-/-}$ mice than *Mmp9*$^{+/+}$ littermates, whereas such a reduction was not observed in *Mmp7*$^{-/-}$ mice (Fig. 4*C*). Notably, almost all metastatic foci in the *Mmp2*$^{-/-}$ and *Mmp9*$^{-/-}$ mice consisted of smaller cancer glands than those in wild-type mice, although they were associated with the iMCs (Fig. 4*D*). These results suggest that MMP2 and MMP9 are critical for the iMCs to promote metastatic expansion of colon cancer cells, but not to accumulate in the liver.

Some Human Colon Cancer Cells Express CCR1 Ligand CCL15. To test whether human colon cancer cells could recruit iMCs, we injected four cell lines into the spleen of *nu/nu* mice and found that HT29 cells were associated with the iMCs in the liver, whereas HCT116, DLD-1, or SW620 cells were not (Fig. 5*A* and Fig. S4*A*). Based on the structural similarity, human orthologs of mouse CCL9 have been suspected to be CCL15 and/or CCL23 (14–16). Thus, we

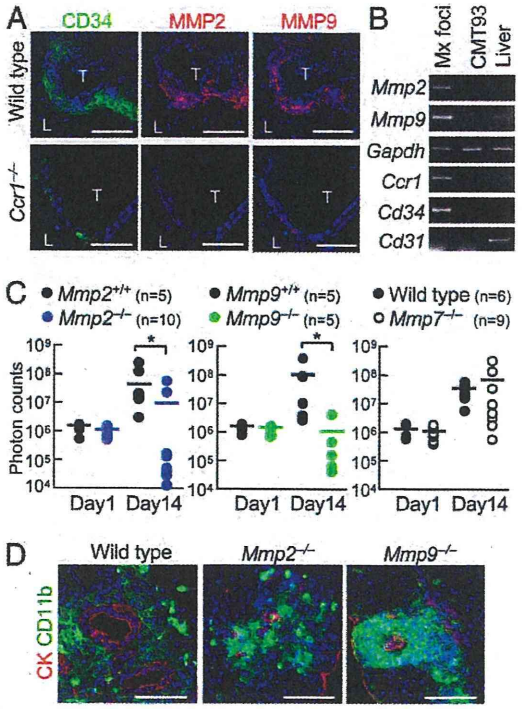

Fig. 4. Lack of MMP2 or MMP9 inhibits expansion of metastatic liver lesions. (*A*) Liver metastasis foci from wild-type and *Ccr1*$^{-/-}$ mice injected with CMT93 cells. Serial sections were stained for CD34, MMP2, and MMP9. T, tumor; L, liver. (Scale bars, 100 μm.) (*B*) Expression of MMP mRNAs determined by RT-PCR. Total RNA was isolated from metastatic foci in wild-type mice (Mx foci), cultured CMT93 cells, and normal mouse liver. Expression of mRNAs for CCR1, CD34, and CD31 were also determined. (*C*) Quantification of metastatic lesions by bioluminescence from luciferase-expressing CMT93 cells. Each circle represents an individual mouse. Horizontal lines show the means of the respective groups. $*P < 0.01$ (n = 9–11 mice in each group). (*D*) Liver metastasis foci in wild-type, *Mmp2*$^{-/-}$, and *Mmp9*$^{-/-}$ mice injected with CMT93 cells. (Scale bars, 100 μm.)

determined the levels of these chemokines in 11 human colon cancer cell lines, and found that six of them including HT29 expressed *CCL15* mRNA and protein at high levels, but not *CCL23* (Fig. 5*B*, Fig. S4 *B* and *C*, and Table S1). We could not detect mRNAs for any other CCR1 ligands; CCL3, 4, 5, 7, 14, or 16 (Fig. S4*C*). We further verified by Western blotting that 28% (13/47) of human colon cancer specimens expressed CCL15 protein (Fig. 5*C*). An immunostaining analysis also showed that 29% (12/41) of primary tumors and 29% (12/41; a separate combination) of liver metastases expressed CCL15 in the cancer epithelium (Fig. 5*D*). These results demonstrate that a subset of human colon cancer cases secretes CCL15 and suggest that it may recruit CCR1$^+$ human iMCs.

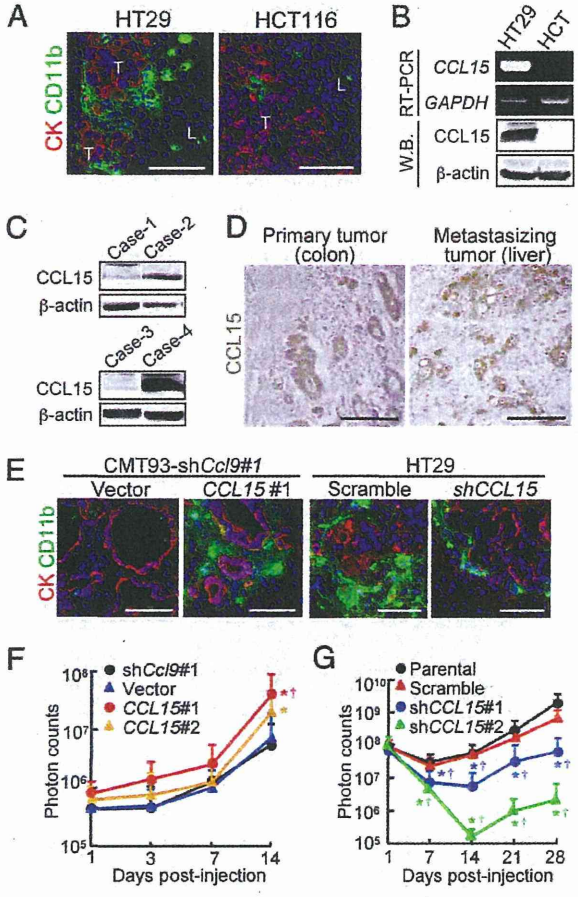

Fig. 5. Human CCL15 recruits the iMCs and promotes expansion of metastatic lesions in mouse liver. (*A*) Liver metastasis foci formed by human colon cancer cells HT29 and HCT116. T, tumor; L, liver. (Scale bars, 100 μm.) (*B*) Levels of CCL15 mRNA and protein determined by RT-PCR and Western blotting, respectively. Total RNA and lysates were prepared from metastatic foci formed by the human colon cancer cell lines in mouse liver. (*C*) Determination of CCL15 protein levels by Western blotting. Lysates were prepared from human colon cancer specimens. Cases-2 and 4 expressed CCL15. β-actin was used as a loading control. (*D*) Human colon cancer specimens immunostained for CCL15 (hematoxylin counterstaining). Tumors were dissected from the primary (colon) and metastatic (liver) sites of the same patients. (Scale bars, 100 μm.) (*E*) Liver metastasis foci from mice with CMT93-sh*Ccl9*#1 cells containing empty vector (Vector) or the *CCL15* gene (*CCL15*#1) (*Left*), and with HT29 cells expressing scramble RNA (HT29-scramble) or shRNA against *CCL15* (HT29-sh*CCL15*) (*Right*). (Scale bars, 100 μm.) (*F*) Quantification of the metastatic lesions in mice injected with CMT93-sh*Ccl9* cells (sh*Ccl9*#1), or their derivatives with empty (Vector) or CCL15-expressing vector (*CCL15*#1 or *CCL15*#2). Results are given as the means ± SD $^*P < 0.04$ and $^\dagger P < 0.03$ compared with sh*Ccl9*#1 and Vector, respectively (n = 5–19 mice in each group). Note that the ordinate is in a logarithmic scale. (*G*) Quantification of the metastatic lesions in mice injected with luciferase-expressing HT29 cells (Parental), or their derivatives expressing scramble RNA (Scramble) or shRNA constructs against *CCL15* (sh*CCL15*#1 or sh*CCL15*#2). Results are given as the means ± SD $^*P < 0.04$ and $^\dagger P < 0.04$ compared with Parental and Scramble, respectively (n = 6–12 mice in each group).

Human CCL15 Promotes Accumulation of the iMCs and Expansion of Metastatic Foci in Mouse Liver. To assess the role of human CCL15 in iMC accumulation and following metastatic expansion of cancer in the liver, we constructed derivatives of the CMT93-sh*Ccl9*#1 cells where not only mouse CCL9 expression was suppressed by an shRNA, but also human *CCL15* was introduced. These cells secreted essentially the same level of CCL15 as those by HT29 cells (321 ± 16, 315 ± 34, and 302 ± 18 pg/10^5 cells for CMT-sh*Ccl9*:CCL15#1, CMT-sh*Ccl9*:CCL15#2, and HT29, respectively), whereas CMT93-sh*Ccl9*#1 cells with the empty vector (CMT-sh*Ccl9*:Vector) did not at any detectable levels. As expected, iMC accumulation was blocked in the majority of metastatic foci formed by CMT93-sh*Ccl9*:Vector cells. In contrast, numerous iMCs accumulated in most tumors of CMT93-sh*Ccl9*:CCL15#1 cells (Fig. 5*E*). We further found that mice injected with CMT93-sh*Ccl9*:CCL15#1 and CMT-sh*Ccl9*:CCL15#2 cells showed higher luminescence levels in the liver than those with control cells at day 14 (Fig. 5*F*). Of note, forced expression of CCL15 did not affect proliferation of CMT93 cells in culture. We next prepared HT29 cells containing shRNA against human *CCL15* (HT29-sh*CCL15*#1 and HT29-sh*CCL15*#2) where expression of CCL15 was reduced to a negligible level (0.1 ± 0.2 and 4 ± 3 pg/10^5 cells for HT29-sh*CCL15*#1 and HT29-sh*CCL15*#2, respectively). In metastatic foci formed by HT29-sh*CCL15*#1 cells, accumulation of the iMCs was markedly reduced compared with those by HT29-scramble cells (Fig. 5*E*). Furthermore, shRNA against *CCL15* (sh*CCL15*#1 and sh*CCL15*#2) significantly reduced the luminescence levels in mice injected with HT29 cells (Fig. 5*G*). These results indicate that CCL15 secreted from human colon cancer cells can recruit mouse CCR1$^+$ iMCs, and promote their metastatic expansion.

CCR1 Antagonist BL5923 Blocks Metastatic Expansion of Cancer in the Mouse Liver and Prolongs Host Survival. Finally, we evaluated a CCR1 antagonist for its suppressive effects on colon cancer metastasis in the mouse liver dissemination model. We administered BL5923 (ref. 17, and *SI Methods*) or the vehicle to *v*/*v* mice that were injected with mouse (CMT93) or human (HT29) colon cancer cells as described above. Treatment of the host mice with 50 mg/kg of BL5923, but not the vehicle, markedly reduced the accumulation of iMCs around the metastatic foci of CMT93 as well as HT29 (Fig. 6*A*). In mice injected with the luciferase-expressing CMT93 cells, BL5923 (at 50 mg/kg) significantly reduced the luminescence levels at day 14, compared with the markedly increased levels in the vehicle-treated mice (Fig. 6*B* and Fig. S5*A*). A lower dose of the compound (25 mg/kg) was ineffective to block the metastatic expansion. As anticipated, BL5923 did not affect the proliferation rate of CMT93 cells in culture (Fig. S5*B*). Likewise, expansion of HT29 cells in the liver was significantly blocked by treatment with 50 mg/kg of BL5923 (Fig. 6*C* and Fig. S5*C*). In contrast, it did not suppress the metastatic expansion of HCT116 cells that could form metastases without iMC accumulation (Figs. 5*A* and 6*C*), consistent with the mechanism that BL5923 blocks tumor metastasis through CCR1 inhibition in the iMCs. We further found that the BL5923 treatment prolonged the mean survival of the hosts from 37 d postinjection to 62 d and from 84 d to 113 d when CMT93 and HT29 cells were injected, respectively (Fig. 6 *D* and *E*). These results strongly suggest that CCR1 antagonist BL5923 suppresses accumulation of the iMCs and early metastatic expansion of colon cancer, allowing the prolonged host survival.

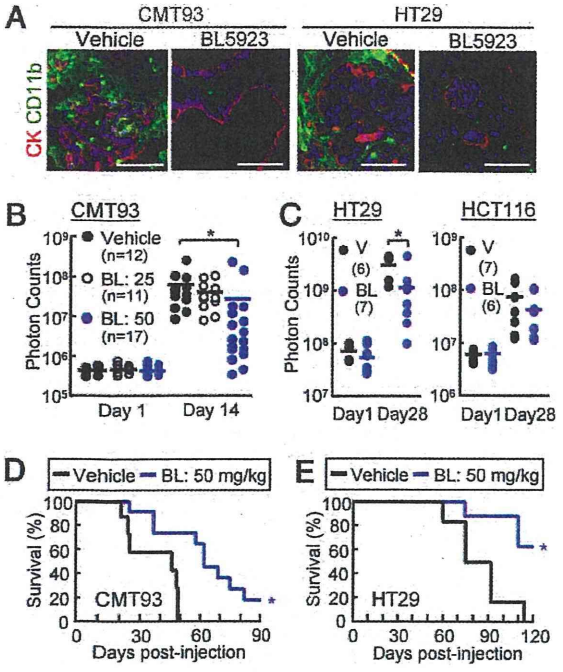

Fig. 6. CCR1 antagonist BL5923 blocks expansion of metastatic lesions and prolongs host survival. (*A*) Liver metastasis foci from mice treated with vehicle or BL5923 (50 mg/kg). Mice were injected with CMT93 cells (*Left*) or HT29 cells (*Right*). (Scale bars, 100 μm.) (*B*) Quantification of metastatic lesions in mice injected with CMT93 cells, and treated with the vehicle or BL5923 at 20 or 50 mg/kg (BL: 25 or BL: 50, respectively). Each circle represents an individual mouse. Horizontal lines show the means of the respective groups. $*P < 0.01$ compared with Vehicle (n = 11–17 mice in each group). (*C*) Quantification of the metastatic lesions in mice treated with vehicle (V) or 50 mg/kg of BL5923 (BL). Mice were injected with HT29 (*Left*) or HCT116 (*Right*) cells. Each circle represents an individual mouse. Horizontal lines show the means of the respective groups. $*P < 0.04$ compared with vehicle (n = 6–7 mice in each group). (*D* and *E*) Kaplan-Meier plots showing survivals of the host mice treated with the vehicle or BL5923 (BL: 50 mg/kg). Mice were injected with CMT93 (*D*) or HT29 (*E*). $*P = 0.004$ compared with vehicle (n = 7–11 mice in each group).

Discussion

In the mouse model, we have found that colon cancer cells disseminated to the liver begin to form micrometastases by day 7 postinjection and rapidly expand thereafter mirroring the extent of iMC accumulation (Figs. 1*B* and 3*B*). Because the disseminated cancer cells cannot expand when the iMC accumulation is blocked, these results suggest that the $CD34^+$ $Gr\text{-}1^-$ iMCs promote a late step of the metastatic cascade: expansion of disseminated cancer and colonization. Because the iMCs have disappeared by day 21 postinjection when cancer cells colonize in the liver, they may support an early phase of metastatic expansion that is rate limiting in the metastatic cascade (18). Consistently, suppression of such early metastatic expansion prolongs survival of mice with disseminated colon cancer in the liver. On the other hand, different subclasses of myeloid cells such as TAMs and $Gr\text{-}1^+$ iMCs help breast cancer cells to invade microvessels, an early step of the metastatic cascade (5–7). However, the $CD34^+$ $Gr\text{-}1^-$ iMCs appear to have only a minor role, if any, in the intravasation and dissemination because the primary colon cancer in *Apc/Smad4* mice do not metastasize despite marked accumulation of the iMCs at the invasion fronts and strong local invasion (10–12).

Interestingly, we have found that CMT93 mouse colon cancer cells recruit the iMCs from the bone marrow to metastatic lesions through the same mechanism as that underlying recruitment of the cells to the primary tumors, activation of CCR1 on the iMCs. Like intestinal tumor epithelium of *Apc/Smad4* mice (12), CMT93 colon cancer cells secrete CCL9, a CCR1 ligand and strong chemoattractant for bone marrow cells (19). Because CMT93 cells do not express other CCR1 ligands (CCL3-CCL7), CCL9 appears to be the only ligand that plays a critical role in recruiting the iMCs. Although human ortholog of mouse CCL9 has not been identified, we have shown here that one-third of human colon cancer metastases express CCL15 that has a structural similarity with CCL9 (14–16). We have further demonstrated that HT29 human colon cancer cells secrete CCL15, recruit mouse iMCs, and expand in the liver, whereas the CCL15-reduced HT29 cells fail to do so. These results suggest that CCL15 secreted from human colon cancer plays a critical role in the recruitment of bone marrow-derived iMCs as a functional homolog of mouse CCL9. Consistently, human CCL15 can promote in vitro migration of mouse mononuclear cells isolated from the bone marrow (20). Although we have been unable to detect CCR1-expressing bone marrow-derived cells in clinical specimens of colon cancer metastasis, it is likely because access is limited only to those in late stages. The transient nature of iMC accumulation in metastasis remains to be investigated further.

In our liver metastasis model, we have found that the iMCs express MMP2 and MMP9, but the tumor epithelium does not. These results are consistent with previous reports that show stroma-restricted expression of the MMPs in human liver metastases of colorectal cancer (21, 22). Abundant expression of MMP2 or MMP9 is associated with poor prognosis and high mortality of colon cancer patients (23–27). Although selective inhibitors of MMP2/9 significantly block mouse liver metastasis of colon cancer and prolong the survival of tumor-bearing mice (28), clinical trials for MMP inhibitors have failed because of severe side effects such as musculoskeletal pain and inflammation (29–31). Alternatively, we have shown here in a mouse model that reduced iMC accumulation by inactivation of CCR1 can suppress metastatic expansion of colon cancer. These results provide the rationale for application of CCR1 antagonists to colon cancer treatment that targets the MMP-expressing myeloid cells, rather than direct and systemic inhibition of MMPs (32). Supporting this novel strategy of "cellular target therapy" (12), we have demonstrated here that CCR1 antagonist BL5923 significantly blocks liver metastasis of mouse (CMT93) and human (HT29) colon cancer cells and prolongs the host survival. Because $Ccr1^{-/-}$ mice are healthy unless challenged with specific pathogens (33), therapeutic inactivation of CCR1 may exhibit few side effects. Consistently, several CCR1 antagonists were well tolerated in phase II trials for rheumatoid arthritis and multiple sclerosis (34). It is therefore possible that administration of CCR1 antagonists as an adjuvant therapy after surgical resection of the primary tumors can improve the survival of patients with colorectal cancer that expresses CCL15. Our present results await clinical trials for such therapies.

Methods

Mice. C57BL/6, $Ccr1^{-/-}$ (33), $Mmp2^{-/-}$ (35), $Mmp7^{-/-}$ (36), $Mmp9^{-/-}$ (37), and *nu/nu* mice at 7 wk of age were used as hosts of tumor injections (see below). All animals were bred and maintained according to the protocol approved by the Animal Care and Use Committee of Kyoto University. Genetic background and origin of the mice are detailed in *SI Methods*.

Cell Lines. CMT93 mouse colon cancer cells (derived from C57BL/6 strain), HT29, DLD-1, SW620, and HCT116 human colon cancer cells were cultured at 37 °C under 5% CO_2 in DMEM with 10% FCS. These cells were transfected with expression vectors encoding luciferase or CCL15, or shRNA expression vectors targeting *Ccl9* and *CCL15* (*SI Methods*).

Clinical Samples. Colon cancer samples for Western blotting were prepared from primary tumors of 47 patients who underwent operations with in-

formed consents. For immunostaining, we prepared an additional 41 sets of the primary colon cancers and liver metastases derived from the same patients.

Experimental Metastasis Model. We injected 1.5×10^6 of CMT93 cells into the spleens of C57BL/6 or knockout mice (C57BL/6 backgrounds) under anesthesia. We also injected 1×10^6 of CMT93 or 3×10^6 of human cancer cells into *nu/nu* mice (*SI Methods*). The spleen was removed 1 min after tumor injection to prevent splenic tumor formation, so that metastatic lesions developed only in the liver.

In Vivo Bioluminescence Imaging. We injected 100 μL of D-luciferin solution (10 mg/mL in PBS, i.p.; Promega) into anesthetized tumor-bearing mice 15 min before imaging. Bioluminescence from the luciferase-expressing tumor cells was determined at days 1, 3, 7, 14, 21, and 28 postinjection, using IVIS-SPECTRUM in vivo photon-counting device (Caliper Life Sciences). Images were quantified as photon counts/second using the Living Image software (Caliper Life Sciences).

Histological Analyses. The methods used for immunostaining were based on those previously described (12). Details are given in *SI Methods*.

Western Blotting. Lysates (50 μg protein each) were separated in 10–20% gradient SDS-gels (WAKO), and Western blotting was performed as described previously (38). CCL15 was detected with a goat polyclonal antibody for human CCL15 (R&D) and Qentix Western Blot Signal Enhancer (Pierce).

RT-PCR. Expression of mRNAs was determined by RT-PCR as described previously (12). Primer sequences are shown in *SI Methods*.

Quantifications of CCL9 and CCL15 Proteins. Conditioned media were collected from cultured CMT93 and HT29 cells, and their derivatives. The levels of CCL9 (MIP-1γ), and CCL15 (MIP-1δ) were determined using the Mouse MIP-1γ Immunoassay Kit, and Human CCL15/MIP-1δ DuoSet ELISA Development Kit (R&D), respectively.

Drug Treatment. BL5923 (Novartis) was dissolved in 0.5% (wt/vol) hydroxyethyl cellulose (17), and administered to mice twice daily by oral gavages at doses of 25 or 50 mg/kg. The relevant solvent was administered to control animals. The treatments were started at 3 d before tumor injection, and continued to the end of analyses.

Statistical Analyses. Statistical significance was evaluated with the Student's *t* test or nonparametric Wilcoxon *u* test. The log-rank test was used for analysis of Kaplan-Meier survival curves. All statistical analyses were performed with JMP 7 (SAS Institute). $P < 0.05$ was considered as statistically significant. Data represent the means ± SD.

ACKNOWLEDGMENTS. We thank M. Okabe (Osaka University) for EGFP transgenic mice, P. M. Murphy (National Institutes of Health) for *Ccr1* knockout mice, and Z. Werb (University of California, San Francisco), S. Itohara [The Institute of Physical and Chemical Research (Japan) Brain Science Institute], and C. Takahashi (Kyoto University) for *Mmp2* and *Mmp9* knockout mice. We also thank T. Inai and E. Hirose (Kyushu University) for CMT93 subtypes, T. Sudo (TORAY Industries Inc., Tokyo, Japan) for performing DNA microarray analysis, and Dr. Kawada (Kyoto University) for preparing human specimens. This work was supported by the Jeannik M. Littlefield-American Association for Cancer Research (AACR) Grants in Metastatic Colon Cancer and Grant-in Aid for Scientific Research from the Ministry of Education, Culture, Sports and Technology of Japan (to M.M.T).

1. Jemal A, et al. (2008) Cancer statistics, 2008. *CA Cancer J Clin* 58:71–96.
2. Christofori G (2006) New signals from the invasive front. *Nature* 441:444–450.
3. Smith SC, Theodorescu D (2009) Learning therapeutic lessons from metastasis suppressor proteins. *Nat Rev Cancer* 9:253–264.
4. Joyce JA, Pollard JW (2009) Microenvironmental regulation of metastasis. *Nat Rev Cancer* 9:239–252.
5. Goswami S, et al. (2005) Macrophages promote the invasion of breast carcinoma cells via a colony-stimulating factor-1/epidermal growth factor paracrine loop. *Cancer Res* 65:5278–5283.
6. Wyckoff JB, et al. (2007) Direct visualization of macrophage-assisted tumor cell intravasation in mammary tumors. *Cancer Res* 67:2649–2656.
7. Yang L, et al. (2008) Abrogation of TGF β signaling in mammary carcinomas recruits Gr-1+CD11b+ myeloid cells that promote metastasis. *Cancer Cell* 13:23–35.
8. Kaplan RN, et al. (2005) VEGFR1-positive haematopoietic bone marrow progenitors initiate the pre-metastatic niche. *Nature* 438:820–827.
9. Gadea BB, Joyce JA (2006) Tumour-host interactions: Implications for developing anticancer therapies. *Expert Rev Mol Med* 8:1–32.
10. Takaku K, et al. (1998) Intestinal tumorigenesis in compound mutant mice of both *Dpc4* (*Smad4*) and *Apc* genes. *Cell* 92:645–656.
11. Taketo MM, Edelmann W (2009) Mouse models of colon cancer. *Gastroenterology* 136:780–798.
12. Kitamura T, et al. (2007) SMAD4-deficient intestinal tumors recruit $CCR1^+$ myeloid cells that promote invasion. *Nat Genet* 39:467–475.
13. Balkwill F (2004) Cancer and the chemokine network. *Nat Rev Cancer* 4:540–550.
14. Wang W, Bacon KB, Oldham ER, Schall TJ (1998) Molecular cloning and functional characterization of human MIP-1 δ, a new C-C chemokine related to mouse CCF-18 and C10. *J Clin Immunol* 18:214–222.
15. Zlotnik A, Morales J, Hedrick JA (1999) Recent advances in chemokines and chemokine receptors. *Crit Rev Immunol* 19:1–47.
16. Forssmann U, Mägert H-J, Adermann K, Escher SE, Forssmann W-G (2001) Hemofiltrate CC chemokines with unique biochemical properties: HCC-1/CCL14a and HCC-2/CCL15. *J Leukoc Biol* 70:357–366.
17. Revesz L, et al. (2006) Bridged piperazines and piperidines as CCR1 antagonists with oral activity in models of arthritis and multiple sclerosis. *Lett Drug Des Discov* 3:689–694.
18. Chambers AF, Groom AC, MacDonald IC (2002) Dissemination and growth of cancer cells in metastatic sites. *Nat Rev Cancer* 2:563–572.
19. Yang M, Odgren PR (2005) Molecular cloning and characterization of rat CCL9 (MIP-1γ), the ortholog of mouse CCL9. *Cytokine* 31:94–102.
20. Kominsky SL, Abdelmagid SM, Doucet M, Brady K, Weber KL (2008) Macrophage inflammatory protein-1 δ: A novel osteoclast stimulating factor secreted by renal cell carcinoma bone metastasis. *Cancer Res* 68:1261–1266.
21. Théret N, et al. (1997) Overexpression of matrix metalloproteinase-2 and tissue inhibitor of matrix metalloproteinase-2 in liver from patients with gastrointestinal adenocarcinoma and no detectable metastasis. *Int J Cancer* 74:426–432.
22. Zeng ZS, Guillem JG (1995) Distinct pattern of matrix metalloproteinase 9 and tissue inhibitor of metalloproteinase 1 mRNA expression in human colorectal cancer and liver metastases. *Br J Cancer* 72:575–582.
23. Cho YB, et al. (2007) Matrix metalloproteinase-9 activity is associated with poor prognosis in T3-T4 node-negative colorectal cancer. *Hum Pathol* 38:1603–1610.
24. Hilska M, et al. (2007) Prognostic significance of matrix metalloproteinases-1, -2, -7 and -13 and tissue inhibitors of metalloproteinases-1, -2, -3 and -4 in colorectal cancer. *Int J Cancer* 121:714–723.
25. Sutnar A, et al. (2007) Clinical relevance of the expression of mRNA of MMP-7, MMP-9, TIMP-1, TIMP-2 and CEA tissue samples from colorectal liver metastases. *Tumour Biol* 28:247–252.
26. Langers AMJ, et al. (2008) MMP-2 geno-phenotype is prognostic for colorectal cancer survival, whereas MMP-9 is not. *Br J Cancer* 98:1820–1823.
27. Inafuku Y, et al. (2009) Matrix metalloproteinase-2 expression in stromal tissues is a consistent prognostic factor in stage II colon cancer. *Cancer Sci* 100:852–858.
28. Wagenaar-Miller RA, Gorden L, Matrisian LM (2004) Matrix metalloproteinases in colorectal cancer: Is it worth talking about? *Cancer Metastasis Rev* 23:119–135.
29. Coussens LM, Fingleton B, Matrisian LM (2002) Matrix metalloproteinase inhibitors and cancer: Trials and tribulations. *Science* 295:2387–2392.
30. Egeblad M, Werb Z (2002) New functions for the matrix metalloproteinases in cancer progression. *Nat Rev Cancer* 2:161–174.
31. Overall CM, Kleifeld O (2006) Tumour microenvironment—opinion: Validating matrix metalloproteinases as drug targets and anti-targets for cancer therapy. *Nat Rev Cancer* 6:227–239.
32. Kitamura T, Taketo MM (2007) Keeping out the bad guys: Gateway to cellular target therapy. *Cancer Res* 67:10099–10102.
33. Gao J-L, et al. (1997) Impaired host defense, hematopoiesis, granulomatous inflammation and type 1-type 2 cytokine balance in mice lacking CC chemokine receptor 1. *J Exp Med* 185:1959–1968.
34. Ribeiro S, Horuk R (2005) The clinical potential of chemokine receptor antagonists. *Pharmacol Ther* 107:44–58.
35. Itoh T, et al. (1997) Unaltered secretion of β-amyloid precursor protein in gelatinase A (matrix metalloproteinase 2)-deficient mice. *J Biol Chem* 272:22389–22392.
36. Wilson CL, Heppner KJ, Labosky PA, Hogan BLM, Matrisian LM (1997) Intestinal tumorigenesis is suppressed in mice lacking the metalloproteinase matrilysin. *Proc Natl Acad Sci USA* 94:1402–1407.
37. Vu TH, et al. (1998) MMP-9/gelatinase B is a key regulator of growth plate angiogenesis and apoptosis of hypertrophic chondrocytes. *Cell* 93:411–422.
38. Fujishita T, Aoki K, Lane HA, Aoki M, Taketo MM (2008) Inhibition of the mTORC1 pathway suppresses intestinal polyp formation and reduces mortality in ApcDelta716 mice. *Proc Natl Acad Sci USA* 105:13544–13549.

Published OnlineFirst on January 11, 2011; DOI:10.1158/0008-5472.CAN-10-2842

Cancer Research

Suppression of Colonic Polyposis by Homeoprotein CDX2 through its Nontranscriptional Function that Stabilizes p27 Kip1

Koji Aoki, Fumihiko Kakizaki, Hiromi Sakashita, et al.

Cancer Res Published OnlineFirst January 11, 2011.

Published OnlineFirst on January 11, 2011; DOI:10.1158/0008-5472.CAN-10-2842

Tumor and Stem Cell Biology

Cancer Research

Suppression of Colonic Polyposis by Homeoprotein CDX2 through its Nontranscriptional Function that Stabilizes $p27^{Kip1}$

Koji Aoki[1], Fumihiko Kakizaki[1], Hiromi Sakashita[2], Toshiaki Manabe[2], Masahiro Aoki[1], and Makoto M. Taketo[1]

Abstract

Caudal-related homeoprotein CDX2 is expressed in intestinal epithelial cells, in which it is essential for their development and differentiation. A tumor suppressor function is suggested by evidence that CDX2 levels are decreased in human colon cancer specimens and that an inactivating mutation of *Cdx2* in $Apc^{\Delta 716}$ mice markedly increases the incidence of colonic polyps. In this study, we investigated roles for transcriptional and nontranscriptional functions of CDX2 in suppression of colonic tumorigenesis. Mutagenic analysis of CDX2 revealed that loss of function stabilizes CDK inhibitor $p27^{Kip1}$ by a nontranscriptional but homeodomain-dependent mechanism that inhibits cyclin E-CDK2 activity and blocks G0/G1-S progression in colon cancer cells. $p27^{Kip1}$ stabilization was mediated by an inhibition of ubiquitylation-dependent proteolysis associated with decreased phosphorylation of Thr187 in $p27^{Kip1}$. siRNA-mediated knockdown of $p27^{Kip1}$ relieved the decrease in cyclin E-CDK2 activity and S-phase cell fraction elicited by CDX2 expression. Together, these results implicate a nontranscriptional function of CDX2 in tumor suppression mediated by $p27^{Kip1}$ stabilization. Up to approximately 75% of low-CDX2 human colon cancer lesions show reduced levels of $p27^{Kip1}$, whereas approximately 68% of high-CDX2 lesions retain expression of $p27^{Kip1}$. These results show that low levels of CDX2 accelerate colon tumorigenesis by reducing $p27^{Kip1}$ levels. *Cancer Res; 71(2); 593–602. ©2011 AACR.*

Introduction

Homeobox transcription factor CDX2 is a mammalian homologue of *Drosophila* caudal that induces the anteroposterior axis (1, 2). In mammalian embryogenesis, CDX2 is essential for self-renewal of the trophoblast cells (3), anteroposterior patterning of the vertebrae, and development of the intestines (4, 5). In adults, CDX2 is expressed specifically in the intestinal epithelium (Fig. 1A; refs. 1, 6), and induces expression of digestive enzymes, adhesion proteins, and transporters (7). In mice, homozygous *Cdx2* mutation causes embryonic lethality whereas the heterozygotes show developmental anomalies, including gastrointestinal hamartomas (4, 5). Consistently, development and differentiation of the intestinal epithelial cells are blocked by homozygous deletion of *Cdx2* in developing intestines (8, 9). These results indicate that CDX2 plays key roles in development and differentiation of colonic epithelial cells.

The levels of CDX2 are reduced in most human colon cancer tissues (10, 11), and in colonic polyps of the $Apc^{+/\Delta 716}$ ($Apc^{+/-}$) mutant mice, a model for human familial adenomatous polyposis (12, 13). The $Cdx2^{+/-}$ mutation increases the colonic polyp number approximately 6 times in $Apc^{+/-}$ mice (Fig. 1B; ref. 12), and accelerates colonic tumorigenesis induced by azoxymethane treatment (14). In mice, and in human and rat colon cancer cell lines, reduced levels of CDX2 stimulate G1-S cell-cycle progression and increase chromosomal instability (12). These results suggest that reduced levels of CDX2 accelerate colonic tumorigenesis. However, the mechanism has been unknown, and its target gene that can suppress tumorigenesis unidentified. To investigate its transcriptional and possibly nontranscriptional functions in the suppression of colonic tumorigenesis, we have performed a mutagenesis analysis of the CDX2 homeodomain (HD) and deletion studies of the protein. We have found that CDX2 has a HD-mediated, but nontranscriptional activity that is sufficient for blocking G1-S progression in the colonic epithelial cell cycle through stabilization of $p27^{Kip1}$ protein. These results suggest a novel nontranscriptional mechanism through which CDX2 suppresses colonic tumorigenesis.

Authors' Affiliations: [1]Department of Pharmacology, Graduate School of Medicine, Kyoto University, and [2]Laboratory of Diagnostic Pathology, Kyoto University Hospital, Kyoto, Japan.

Note: Supplementary data for this article are available at Cancer Research Online (http://cancerres.aacrjournals.org/).

Corresponding Author: Makoto Mark Taketo, Department of Pharmacology, Graduate School of Medicine, Kyoto University, Yoshida-Konoé-cho, Sakyo-ku, Kyoto 605-8501, Japan. Phone: 81-75-753-4391; Fax: 81-75-753-4402. E-mail: taketo@mfour.med.kyoto-u.ac.jp

doi: 10.1158/0008-5472.CAN-10-2842

Published OnlineFirst on January 11, 2011; DOI:10.1158/0008-5472.CAN-10-2842

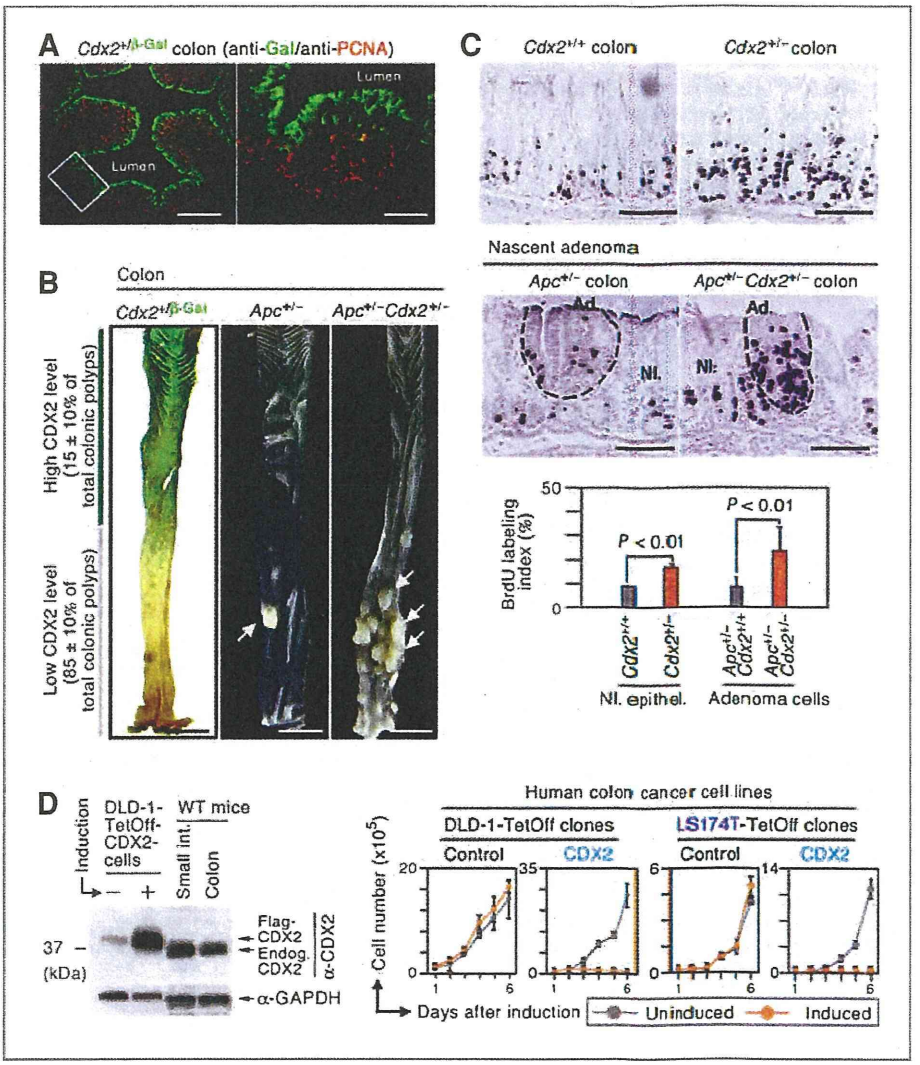

Figure 1. CDX2 blocks cell proliferation of normal, adenoma, and carcinoma epithelia of colon. A, relationship between CDX2 expression (green) and proliferation (red) in colonic epithelial cells in a cross section at low magnification (left). The colon of *Cdx2*–β-Gal (β-galactosidase) knock-in mice ($Cdx2^{+/\beta\text{-Gal}}$) were stained with antibodies for β-Gal (green) and PCNA (a marker for cell proliferation, red), simultaneously. Right, a higher magnification of the boxed area in the left. Magnification bars, 400 μm (left) and 100 μm (right). B, representative photographs of LacZ-stained $Cdx2^{+/\beta\text{-Gal}}$ colon (left), and nonstained colons of $Apc^{+/-}$ (center) and $Apc^{+/\Delta 716}Cdx2^{+/\beta\text{-Gal}}$ ($Apc^{+/-}Cdx2^{+/-}$; right). Scale bars, 1 cm. Note that approximately 85% of polyps in $Apc^{+/-}$ and $Apc^{+/-}Cdx2^{+/-}$ were found in the distal region where the level of CDX2 was lowest. Polyp distribution with SD were from 4 $Apc^{+/-}$ and 4 $Apc^{+/-}Cdx2^{+/-}$ mice at 10 weeks of age. Arrows point to representative colonic polyps in the large-size class. C, representative photographs of colonic epithelial cells labeled with BrdU in wild-type ($Cdx2^{+/+}$) and $Cdx2^{+/-}$ mice (top), and those of adenoma cells in nascent polyps of $Apc^{+/-}$ and $Apc^{+/-}Cdx2^{+/-}$ mice (middle) at 10 weeks of age. Quantified data from 3 mice are shown with SD (bottom). Nl., normal colonic mucosa; Ad., adenoma cells; Epithel., epithelial cells. Magnification bars, 100 μm. D, induction of Flag-tagged CDX2 in DLD-1–TetOff cells analyzed by Western blotting (WB; left), compared with that in lysates prepared from intestines (int.) of wild-type mouse. Glyceraldehyde 3 phosphate dehydrogenase (GAPDH) was used as a loading control. Note that induced Flag-CDX2 shows slower migration than endogenous (endog.) CDX2, due to its Flag tag. Proliferation profiles of DLD-1–TetOff and LS174T–TetOff cell clones that induced expression of CDX2 are shown with SD, compared with uninduced cells (right).

Materials and Methods

BrdU labeling, X-gal staining, determination of polyp distribution, and human tissue samples

The $Apc^{+/-}$, $Cdx2^{+/\beta\text{-Gal}}$ ($Cdx2^{+/-}$), and $Apc^{+/-}Cdx2^{+/-}$ mice have been described previously (5, 12, 13). Bromodeoxyuridine (BrdU) labeling and X-gal staining were carried out as described previously (5, 12). All animal experiments were approved by the Animal Care and Use Committee of Kyoto University. Colonic polyps in the $Apc^{+/-}$ and $Apc^{+/-}Cdx2^{+/-}$ mice (4 mice at the age of 10 weeks, respectively) were scored as described previously (12). Human tissue samples and

Published OnlineFirst on January 11, 2011; DOI:10.1158/0008-5472.CAN-10-2842

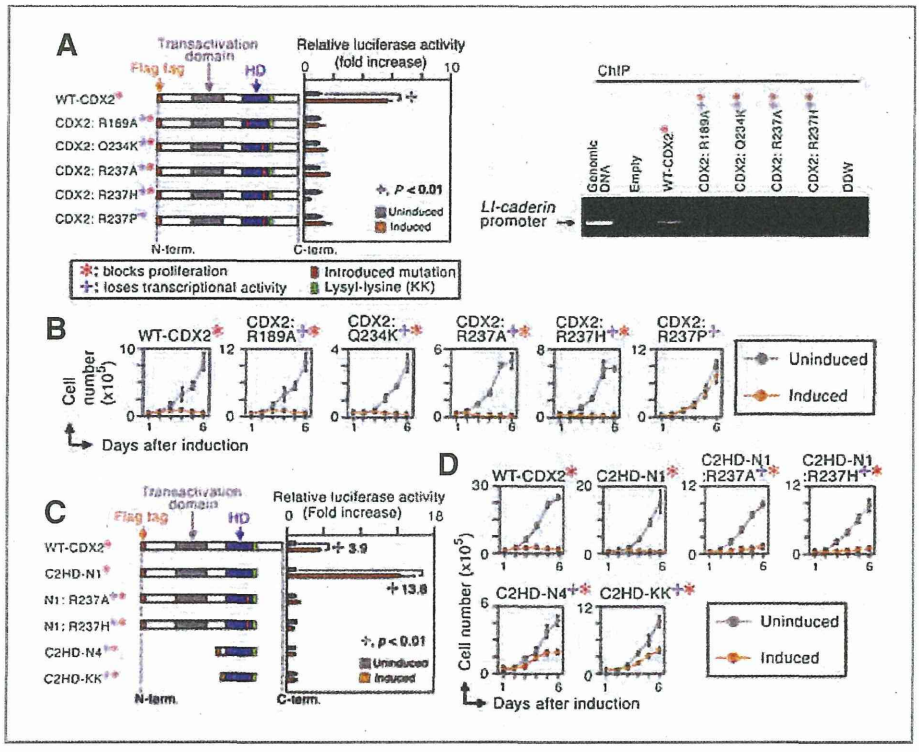

Figure 2. Nontranscriptional activity of CDX2 in N-terminal (N-term.) and homeobox domains is sufficient to block cell proliferation. A, schematic representation of transcription-defective CDX2 mutant proteins (left). Transcriptional activities of the respective mutant CDX2 proteins were determined on day 2 of induction in DLD-1–TetOff clones, using a luciferase reporter carrying a promoter region of the *LI-cadherin* gene (left). The activities are shown with SD. Lack of DNA-binding activity of CDX2 mutant proteins was also analyzed by chromatin immunoprecipitation assay (ChIP) for the *LI-cadherin* gene promoter (right). Genomic DNA was used as a positive control. C-term, C-terminal. B, proliferation profiles of DLD-1–TetOff cells on induction of transcription-defective CDX2 mutant proteins, compared with uninduced cells. The mean cell numbers are shown with SD. C, schematic representation of CDX2 deletion mutant proteins (left). Transcriptional activities of the respective mutant CDX2 proteins were determined on day 2 of induction in DLD-1–TetOff clones, using a luciferase reporter carrying a promoter region of the *LI-cadherin* gene (right). The activities are shown with SD. Right, numbers indicate relative ratios of the induced to the uninduced activities. D, proliferation profiles of DLD-1–TetOff cells on induction of CDX2 deletion mutant proteins, compared with uninduced cells. The mean cell numbers are shown with SD.

immunohistochemical analysis are described in Supplementary Data.

TetOff system and introduction of small interfering RNA into TetOff cells

TetOff cells were generated, using a pTetOff vector (Clontech). CDX2 and its mutants were expressed in the respective stable TetOff cell clones, using a pTRE-Tight vector (Clontech). Introduction of small interfering RNA duplexes (siRNA) into TetOff cells and siRNA used in this study, and cell-proliferation assay are described in Supplementary Data.

Mutagenesis of CDX2 HD and construction of CDX2 deletion mutants

Mutagenesis of the CDX2 HD was carried out using QuickChange II Site-Directed Mutagenesis Kit (Stratagene), and confirmed by sequencing. Deletion mutants of CDX2 were constructed by PCR. Sequences of oligonucleotides used for the mutagenesis and for construction of the deletion mutants are provided in Supplementary Data. Construction of luciferase reporters and chromatin immunoprecipitation analysis are also described in Supplementary Data (15).

Immunoprecipitation, Western blotting, and cycloheximide chase

Analyses of the $p27^{Kip1}$ complex and its subcelluar localization are described in Supplementary Data. For analysis of the $p27^{Kip1}$ ubiquitylation, cells were treated with 10 μmol/L of MG132 (Sigma-Aldrich) for 12 hours.

For analysis of $p27^{Kip1}$ protein stabilization, cells were treated with 100 μg/mL of cycloheximide (CHX; Sigma-Aldrich). Quantitative RT-PCR analysis for the *CDKN1B* mRNA is also described in Supplementary Data.

Statistical analysis

Statistical analyses were carried out by the Student's *t* test to compare the mean (Figs. 1, 2, and 4), or by the χ^2 test to compare the CDX2 and $p27^{Kip1}$ levels in human colon cancer specimens (Fig. 6), using JMP software (SAS Institute Japan). $P < 0.05$ was considered significant.

Published OnlineFirst on January 11, 2011; DOI:10.1158/0008-5472.CAN-10-2842

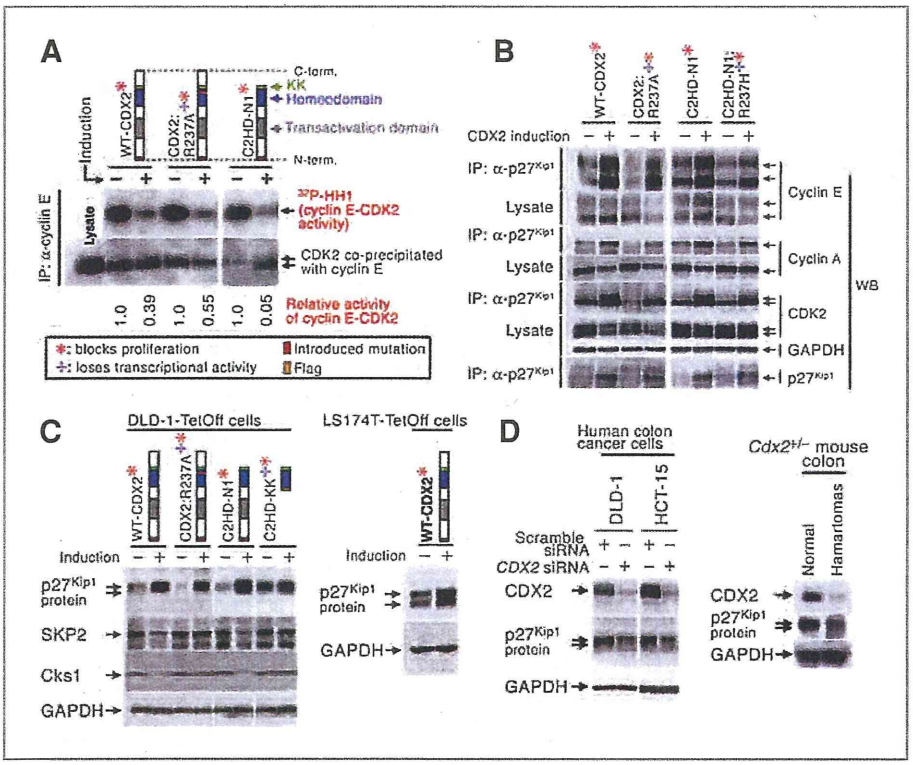

Figure 3. CDX2 increases amounts of $p27^{Kip1}$ protein and cyclin-CDK2/$p27^{Kip1}$ complex. A, kinase activity of CDK2 coimmunoprecipitated with cyclin E (IP; anti-cyclin E) on histone H1 (HH1) substrate on day 2 of induction of wild-type or mutant CDX2 in DLD-1–TetOff cells, analyzed by *in vitro* kinase assay. The ^{32}P incorporation into HH1 is shown (top). The level of CDK2 coimmunoprecipitated with cyclin E was also analyzed by Western blotting (bottom). The relative kinase activities of cyclin E-CDK2 are shown beneath the gel photo. The faster-migrating band of CDK2 corresponds to the protein phosphorylated only at T160 that is essential for its activation, whereas the slower band represents CDK2 phosphorylated at inhibitory phosphorylation sites Y14 and T15 (41). C-term, C-terminal; N-term, N-terminal. B, amounts of cyclin E, cyclin A, and CDK2 coimmunoprecipitated with $p27^{Kip1}$ analyzed by immunoprecipitation assay (IP), on day 2 of induction of wild-type CDX2 or its mutants in the DLD-1–TetOff clones. Amounts of the cyclins and CDK2 coimmunoprecipitated with $p27^{Kip1}$, and their lysate levels were analyzed by Western blotting (WB). Glyceraldehyde 3 phosphate dehydrogenase (GAPDH) was used as a loading control, and precipitated $p27^{Kip1}$ is also shown. C, amounts of $p27^{Kip1}$, SKP2, and Cks1 proteins on day 2 of induction of wild-type or mutant CDX2 in DLD-1–TetOff (left) and in LS174T–TetOff cell clones (right), analyzed by Western blotting. GAPDH was used as a loading control. Double bands of $p27^{Kip1}$ protein have been described (42). D, amount of $p27^{Kip1}$ protein on day 2 after introduction of siRNA against *CDX2* in human colon cancer cell lines DLD-1 and HCT-15, analyzed by Western blotting (left). Reduced level of CDX2 is shown on the top (left). Amount of $p27^{Kip1}$ protein in colonic hamartomas of the $Cdx2^{+/-}$ mutant mice was analyzed by Western blotting (right). GAPDH was used as a loading control. Note essentially absent CDX2 in the hamartomas (right, top). Normal, the lysate derived from the surrounding normal mucosa.

Results

CDX2 blocks cell proliferation of normal, adenoma and carcinoma epithelia of colon

In the colonic epithelium, CDX2 was expressed strongly in the nonproliferating differentiated cells, whereas its level in the proliferating cells was much lower (Fig. 1A; ref. 6). The $Cdx2^{+/-}$ mutation increased proliferation of normal colonic epithelial cells by approximately 2 times (Fig. 1C, top) and of adenoma cells by approximately 3 times (Fig. 1C, middle). These results suggest that CDX2 normally suppresses proliferation of normal and adenoma epithelial cells of the colon. Consistently, most colonic polyps were found in the distal region where the level of CDX2 was low, in both $Apc^{+/-}$ and $Apc^{+/-}Cdx2^{+/-}$ mutant mice (Fig. 1B; 79 ± 8% and 92 ± 8%, respectively; mean ± SD).

To investigate the mechanism by which CDX2 suppressed the proliferation, we constructed doxycycline-controlled "Tet-Off–CDX2" cell clones, in which CDX2 was induced at levels comparable to those in the normal intestines (Fig. 1D, left). As test cells, we chose near-diploid human colon cancer lines DLD-1 and LS174T, which were used as models for the intestinal progenitor cells (16) and expressed low levels of CDX2 (Fig. 1D, left). In these cell lines, Wnt signaling is activated through mutations in the *APC* and β-catenin genes, respectively. In addition, both Ras and phosphatidylinositol-3 kinase (PI3K)-Akt signaling pathways are also activated by mutations in *KRAS* and *PIK3CA* genes (17), whereas p53 is mutated only in DLD-1 cells.

As expected, induction of CDX2 in the TetOff cells caused 2 to 3 times higher transcriptional activities as determined by luciferase reporters carrying promoters for the *LI-cadherin*